5: Investigation of the iHO luminal response to infection, iHO as a model for alternative pathogens, competition between bacterial strains and interactions of *Salmonella* with iHO derived from cell lines with isogenic mutations

Collaboration note:

The data in this chapter on *Salmonella enterica* serovar Enteritidis (*S*. Enteritidis) were generated jointly with Rafal Kolenda, a PhD student from the University of Wrocław whom I taught how to generate iHO and complete intracellular and luminal infection assays.

5.1 Introduction

As detailed in Chapter 4, it was possible to demonstrate an enhanced barrier phenotype associated with iHO in response to IL-22. Additionally, whilst we identified a mechanism for intracellular protection following IL-22 stimulation, further questions can potentially be answered using this system. Compared to 2-D cell culture, the iHO model incorporates more components of the intestinal luminal environment found *in vivo*. The use of microinjection, allows the introduction of pathogens into a closed system, which reproduces aspects of the intestinal luminal environment and allows controlled observations to be made. For example, studies on *Helicobacter pylori* in gastric organoids were able to demonstrate that bacteria were attracted to the urea being produced by the gastric organoid epithelial cells, and the bacteria were able to use this signal to locate the epithelium for binding and subsequent colonisation.[1] Similarly, other studies using gastric organoids were able to demonstrate that parietal cells (which are difficult to maintain in monolayer culture but viable within the organoid structure), were responsible for Sonic hedgehog (Shh) production, which is a factor that induces macrophage infiltration post-infection.[2] More specifically to the small intestinal organoid model, studies have attempted to look at α-defensin concentrations following secretion by Paneth cells into the organoid lumen, and whether these exist at high enough

concentrations to have a directly antimicrobial effect.[3] These types of question are more difficult to answer *in vivo*, given the multiple interactions with the mucosal immune system and intestinal microbiota.[4] A study in murine intestinal organoids, demonstrated the ability of alpha defensins to restrict growth of strains of *S*. Typhimurium for up to 20 hours after microinjection, with a 3.9-log reduction in bacterial counts versus those seen in organoids derived from $Mmp7^{-/-}$ mice, which lack matrix metalloproteinase 7 and are unable to produce functional α-defensins.[3] Organoids as vessels for infection modeling are growing in use, with pathogens such as *H. pylori*,[5] norovirus,[6] rotavirus,[7] Shiga toxin-producing *Escherichia coli*,[8] Cryptosporidium,[9] and Zika virus[10] having been shown to survive and replicate within these systems.

Having investigated how well *S*. Typhimurium SL1344 invades intracellularly and survives in the lumen of the iHO system, it was of interest to expand this line of enquiry to other serovars of *Salmonella*, such as *S*. *enterica* serovar Enteritidis, which causes both gastrointestinal disease and invasive non-typhoidal salmonellosis (iNTS).[11] Additionally, with the hypothesis that bacteria may be killed by antimicrobial peptides in the iHO lumen, assays were performed to assess this with an attaching and effacing pathogen, Enteropathogenic *E. coli* (EPEC), which would not be expected to extensively reside within cells.[12] We also wished to investigate how drug-resistant isolates of *Salmonella* that cause invasive disease in humans would behave in the iHO model. This is particularly relevant when considering that these isolates have the potential to outcompete other sensitive strains in the microbiota *in vivo*, either within or across species, as suggested by a recent study.[13] A number of Vietnamese clinical strains were therefore put directly in competition with the laboratory reference strain (*S*. Typhimurium SL1344) with the hypothesis that strains causing severe disease in humans may be better able to invade the iHO epithelium. The clinical strains used were a mixture of those expressing monophasic and biphasic flagellae. Flagellar protein (fliC or fljB) is the main structural subunit of the flagellar filament in most *Salmonella* strains,[14] with fliC coding phase 1 flagellins and fljB phase 2 flagellins. FliC is antigenic and is expressed in multiple *Salmonella* serotypes, as well as having a homolog in other pathogens such as *E*. *coli*.[15] FljB is only expressed in *S. enterica* subspecies I, II, IIIb and Vi, and the *fljB* gene is located on a different part of the chromosome to the *fliC* gene.[16] Both flagellin genes are not normally expressed at the same time as biphasic

bacteria display phase variation, switching between the two phases, with the switch controlled by an invertible element called *hin.*[17] (**Figure 5.1**)

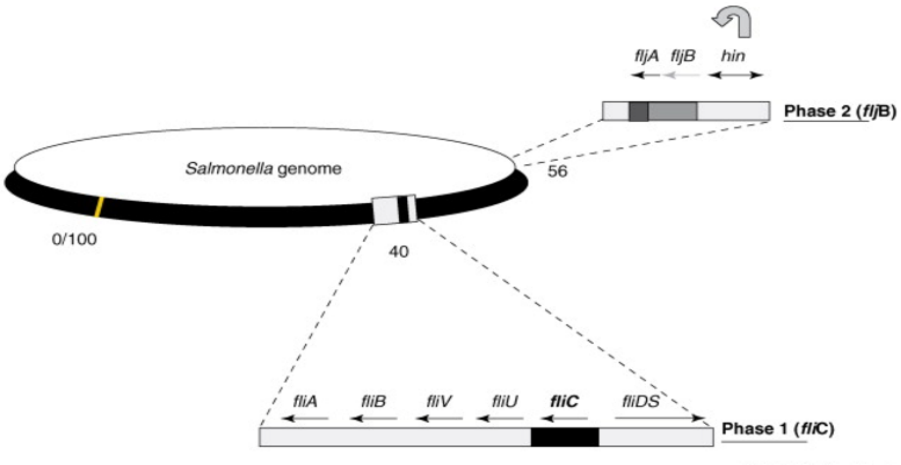

Figure 5.1: Interactions of *fliC* and *fljB* loci. This figure demonstrates the locations on the *Salmonella* genome of the *fliC* and *fljB* loci, as well as the location of the reversible *hin* element which facilitates phase variation. In one orientation, *hin* promotes expression of both *fljB* and the post-transcriptional repressor *fljA,* leading to lack of expression of *fliC*. The converse is true when the orientation of *hin* is reversed. (Figure taken from McQuiston et al, 2008[16])

It is unclear what exactly leads to the phase switch. Some *Salmonella* strains are monophasic, through the loss or deletion of *fljB.* Possible advantages from the biphasic lifestyle could include limited antigenic diversity and temporary evasion of the immune response, or improved adaptation to a particular environmental niche.[16]

Finally, we hypothesised that it would be possible to expand the clinical utility of iHO by deriving them from individuals with mutations in genes involved in the immune response to directly investigate the effect of these mutations on IEC response to infection. To this end, we generated iHO from an individual with a mutation in the caspase recruitment domain-containing protein 8 (CARD8) gene as described below and conducted infection assays in this model using *S*. Typhimurium SL1344.

5.2 Assessing whether luminal bacterial killing occurs in the iHO model

As described in Chapter 4, initial invasion of *S*. Typhimurium SL1344 was restricted in rhIL-22 treated iHO and there was uncertainty about the location of killing of the less invasive strain ST4/74 ΔPhoPQ. Therefore, the question arose of whether there was any luminal killing effect

induced by IL-22 treatment, perhaps mediated by an increased antimicrobial peptide release into the iHO lumen. This was investigated by microinjecting bacteria and harvesting the luminal contents of the iHO at 90 minutes post-infection, as described in 2.3. Initial assays performed with ST4/74 and ST4/74 ΔPhoPQ bacteria at a starting OD_{600} of 1 (1.6 x 10^9 CFU/mL) did not show any significant difference in bacterial counts recovered from the lumen with or without rhIL-22 treatment. To assess whether this could be due to the bacterial inoculum overloading the defensive capacity of the iHO, the assay was expanded by inoculating iHO with *S*. Typhimurium SL1344 at a series of 10-fold dilutions. In these assays, significantly fewer bacteria were recovered from the lumen of rhIL-22 treated iHO compared to unstimulated equivalents at bacterial concentrations of 1.6 x 10^8 CFU/mL and 1.6 x 10^7 CFU/mL (**Figure 5.2**).

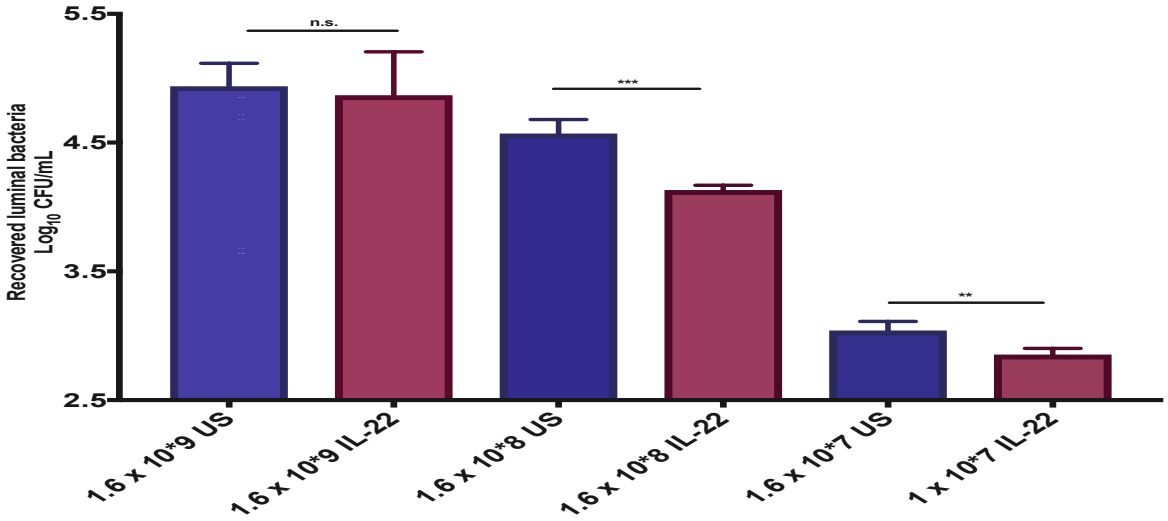

Figure 5.2: Luminal bacterial counts using decreasing SL1344 inoculums in Kolf2 iHO pre-treated with rhIL-22 vs unstimulated (US). iHO were either pre-treated with rhIL-22 at 100 ng/mL for 18 hours or left unstimulated. iHO were injected with a series of 10-fold dilutions of SL1344 and incubated for 1.5 hours prior recovery of intraluminal bacteria. Data presented are for 3 biological replicates (each averaged from 3 technical replicates), with 30 iHO injected per replicate +/- SEM. Unpaired Mann-Whitney tests were used for all assays (n.s. – not significant, ** p< 0.01, *** p < 0.001). There were significantly fewer bacteria recovered from the lumen in iHO pre-treated with rhIL-22 at both of the lower concentrations of bacteria injected.

Luminal killing assays were additionally performed using an *S*. Typhimurium SL1344 *invA* mutant, which has a deletion in the *invA* gene of *Salmonella* pathogenicity island 1. This derivative has been demonstrated to be less invasive in the iHO system,[18] and therefore may remain in the iHO lumen for a longer time before entering the epithelial cells. These assays were performed over a time course with iHO harvested directly after injection and then

hourly for 4 hours. Having observed luminal survival differences at the lower inoculums, the concentration of the bacterial solution used for these assays was 1.6 x 10^8 CFU/mL. For SL1344, there appeared to be some luminal killing effect, with significantly fewer bacteria recovered from the lumen at 1, 2 and 3 hours post injection for those iHO pre-treated with rhIL-22. For SL1344 Δ*invA*, there were significantly fewer bacteria recovered at the 1 hour timepoint following rhIL-22 treatment, but this effect was not obvious from the 2 hour timepoint onwards. It is possible that with increased numbers of bacteria remaining in the lumen, rather than invading, the bacterial load in the lumen was high enough to exceed any killing effect related to IL-22 treatment. Interestingly, for both groups treated with rhIL-22, there were significantly increased counts of bacteria recovered from the lumen at 4 hours, suggesting that the protective effect of IL-22 on luminal bacteria is limited to the early stages of infection (**Figure 5.3**). Perhaps the increased mucus release stimulated by IL-22, whilst preventing entry into cells, provides a niche in which bacteria can replicate. This is discussed further later in the chapter.

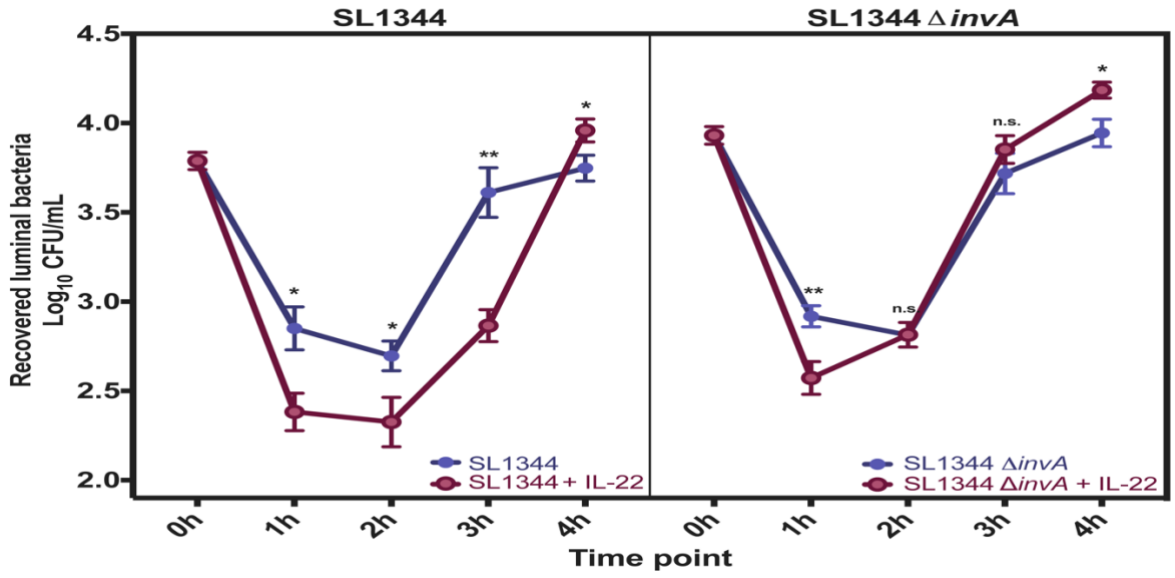

Figure 5.3: Luminal bacterial counts at timepoints following injection of Kolf2 iHO with SL1344 or SL1344 Δ*invA*. iHO were either pre-treated with rhIL-22 at 100 ng/mL for 18 hours or left unstimulated. iHO were injected with SL1344 or SL1344 Δ*invA* at 1.6 x 10^8 CFU/mL and incubated for 0, 1, 2, 3 or 4 hours prior to recovery of intraluminal bacteria. Data presented are for 3 biological replicates (each averaged from 3 technical replicates), with 30 iHO injected per replicate, +/- SEM. Unpaired Mann-Whitney tests were used for all assays (n.s. – not significant, * < p<0.05, ** p< 0.01). There were significantly fewer bacteria recovered from the lumen in rhIL-22-treated iHO for the first 3 hours after injection with SL1344. This effect was only detected for the first hour for SL1344 Δ*invA*-infected iHO.

From these assays it was clear that initially, killing of bacteria in the lumen was occurring, but eventually, significant numbers of bacteria were able to survive and replicate in the lumen, enabling them to invade and damage the iHO epithelium. Imaging of iHO using the Incucyte S3 live cell analysis system (Sartorius) at 3-4 hours post-injection demonstrated clear destruction of iHO tissue (**Figure 5.4**). Bacteria used for imaging in the Incucyte system were TIMER^{bac}-*Salmonella* SL1344,[19] which produce differently coloured fluorophores depending on their growth rate, therefore via measurement of colour change, it was possible to witness bacterial survival and replication in the lumen over time. Green fluorophores are initially produced, which later mature into orange fluorophores. Thus, rapidly dividing cells will fluoresce predominantly green, since the slower maturing orange fluorophores will be diluted by cell division. On sequential imaging, it was possible to view areas where TIMER^{bac}-*Salmonella* SL1344 had been injected into the iHO and observe these infected spots fluorescing green over time as exponential growth phase is reached.

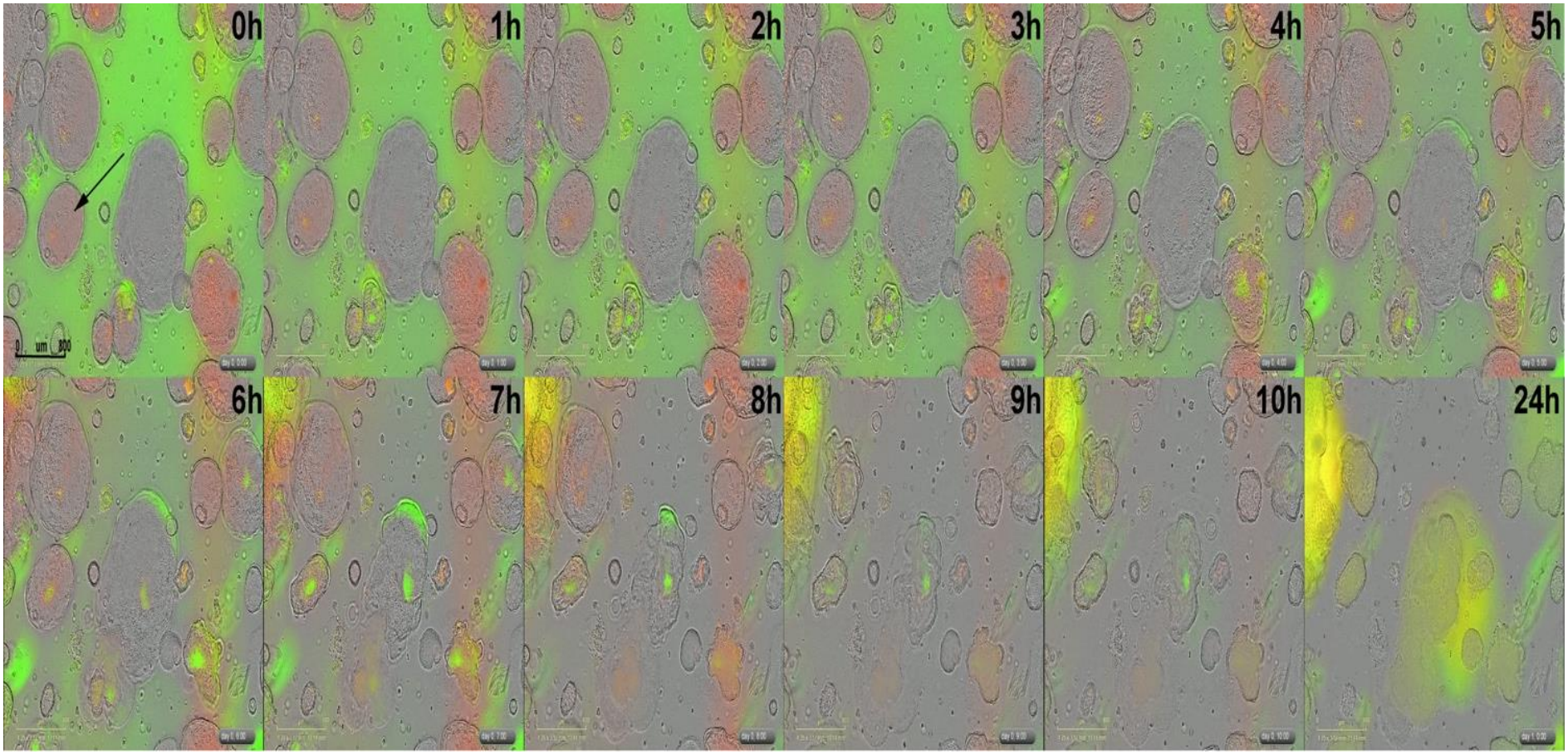

Figure 5.4: Sequential imaging of Kolf2 iHO infected with TIMER^{bac}-*Salmonella* SL1344. Organoids were imaged every 10 minutes for 24 hours following infection with TIMER^{bac}-*Salmonella* SL1344. Injection sites on iHO are visible as green/orange dots (arrow) which initially appear static in terms of growth, but later fluoresce green as bacteria overtake iHO defences and start to replicate rapidly. Visible destruction of the iHO architecture is witnessed between 3 and 4 hours after injection. By 24 hours after infection, iHO are destroyed and bacteria are dividing rapidly in the culture media. Artefactual green background staining in initial images is generated by Matrigel embedding scaffold and red staining by phenol red injected with bacteria. Images taken using the Incucyte S3 system at 4x magnification; scale bar = 800μm.

It was also possible to use these images to measure green and red fluorescence of TIMER^{bac}-*Salmonella* SL1344 over time, for infected unstimulated and rh-IL22-treated iHO. There was no significant difference in groups between green fluorescence, although some initial growth advantage was suggested in the unstimulated group (**Figure 5.5**). Total red fluorescence was significantly higher in the unstimulated group, particularly in the first 8 hours following infection, suggesting a non-replicating cohort of bacteria surviving either in the lumen or intracellularly within unstimulated iHO and bacterial death in the IL-22 stimulated group. Studies of *S*. Typhimurium in human and mouse macrophages have demonstrated a non-replicating subset of bacteria existing intracellularly following infection.[20,21]

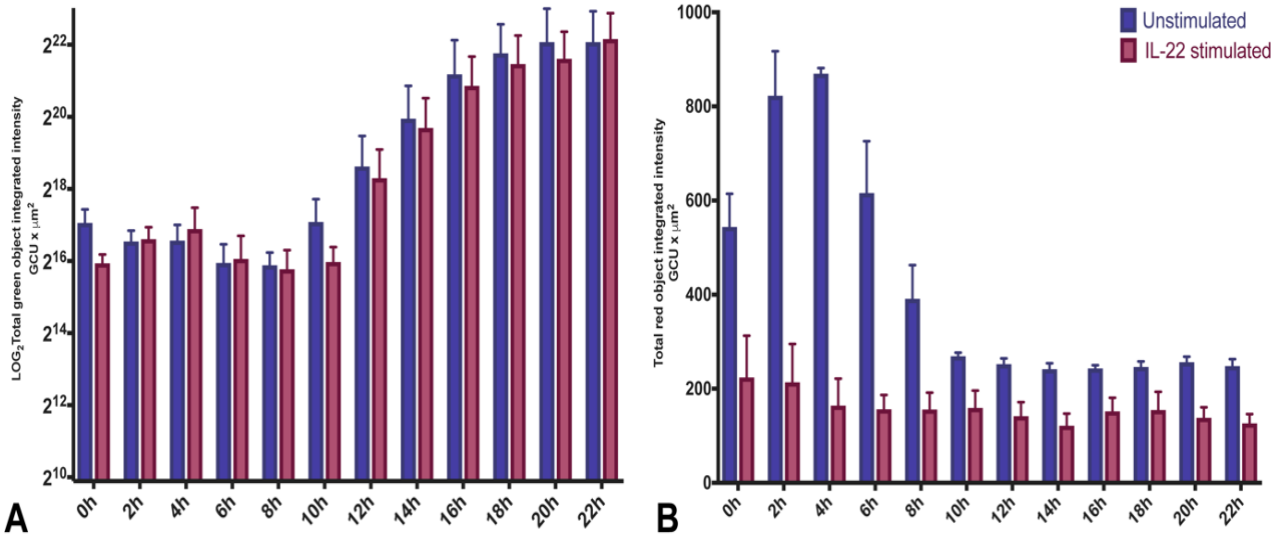

Figure 5.5: Total green / red fluorescence over time for TIMER^{bac}-*Salmonella* SL1344 following Kolf2 iHO infection. iHO were either pre-treated with rhIL-22 at 100 ng/mL for 18 hours or left unstimulated, then injected with TIMER^{bac}-*Salmonella* SL1344 and incubated for 22 hours, and red/green fluorescence recorded over time. Wilcoxon matched pairs signed rank test was used for statistical analysis. There was no significant difference in green fluorescence over time between the two groups (**A**), but significantly higher total red fluorescence in the unstimulated group (**B**) ($p = 0.0005$).

5.3 Reviewing the luminal contents of the iHO and their effects on other bacterial strains

Ideally, study of the intra-luminal AMP contents of the iHO would involve being able to directly extract the luminal contents and run proteomic analysis on them. In lieu of the ability to do this, transcripts for antimicrobial peptides of interest were measured as a proxy. RT-qPCR assays using Taqman reagents were completed for REGIIIα, Lysozyme C

(LYZ), Alpha defensin 5 (DEFA5), Defensin beta 4B (DEFB4B) and Phospholipase A2 group IIA (PLA2G2A). These genes were chosen as they represent a combination of alpha and beta defensins and C-type lectins and would be expected to be upregulated in response to *Salmonella*[22], or *E*. coli infections in iHO.[23] It was not possible to consistently detect transcripts for REGIIIα, even at an increased starting concentration of cDNA (1:50 vs 1:100), therefore these data were excluded from the analysis. iHO were either harvested uninfected (time 0), or infected with SL1344 and harvested at 1, 2 or 3 hours post-infection and RNA extracted (**Figure 5.6**). Transcripts for DEFB4B were significantly upregulated from 1 hour post infection, and DEFA5 from 2 hours post-infection. Basal levels of Lysozyme C were very high (partly to be expected as this AMP should be found in all Paneth cells), therefore no significant difference in its expression across timepoints was observed.

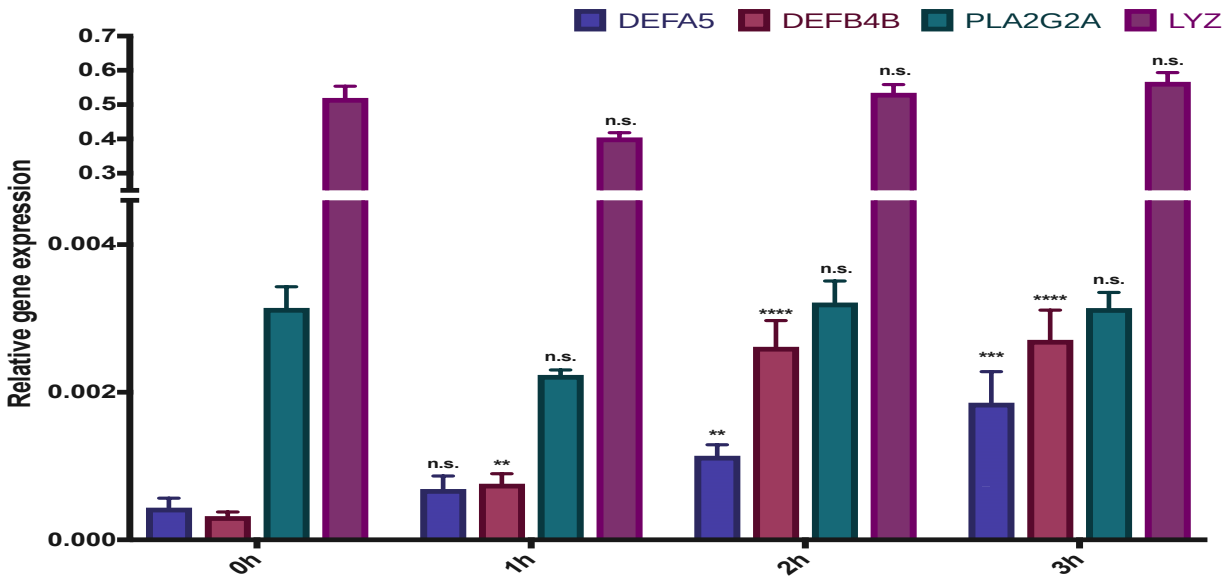

Figure 5.6: Expression of antimicrobial peptides over time following Kolf2 iHO infection with SL1344. iHO were injected with SL1344 and harvested at 0, 1, 2 or 3 hours post-infection, RNA extracted and RT-qPCR completed for AMP transcripts of interest. Data presented are for 3 biological replicates, each averaged from 4 technical replicates. Data were analysed using the comparative cycle threshold (C_T) method, with GAPDH as an endogenous control. Unpaired Mann-Whitney test was used to compare results (**n.s.** not significant, **p <0.01, ***p <0.001, ****p <0.0001). Transcripts for DEFB4B were significantly upregulated from 1 hour post infection, and DEFA5 from 2 hours post-infection.

Having studied a number of strains of *S*. Typhimurium, and witnessed initial drops in luminal bacterial counts before a recovery period, the question arose of whether this pattern would be repeated for other serovars of *Salmonella*. Assays were completed using *S*. Enteritidis strains 6206 and 6174. These were isolates from stool; 6174 from a human sample and 6206

from a poultry sample. *S*. Enteritidis 6174 has a mutation in the gene coding the outer membrane porin protein *ompD*. Previously, *Salmonella* with *ompD* mutations have been shown to have increased ability to survive and replicate within murine organs,[24] and have an increased resistance to beta-lactam antibiotics.[25] *S*. Enteritidis 6206 has a SNP in the N-acetylmuramyl-L-alanine amidase (*amiA*) promoter. *amiA* has a role in cell wall hydrolysis during cell division. *E. coli* with these mutations have been shown to be more susceptible to human neutrophil peptide 1 (HNP-1; a type of alpha-defensin).[26] *S*. Typhimurium SL1344 was used as a control, given that its behaviour in the iHO model had been previously established. In addition, P125109 (PT4); a reference isolate of *S*. Enteritidis[27] frequently used for laboratory work was trialled in the model as a comparator. Single iHO were harvested immediately following infection (time 0), and at hourly timepoints thereafter. SL1344 demonstrated intraluminal survival following an initial drop in viable bacteria as seen previously. Significantly fewer P125109 survived in the lumen, and the luminal bacterial population appeared to be at an equilibrium between rates of replication and death from 2-4 hours. Counts for 6174 and 6206 consistently decreased over time, suggesting intraluminal killing; particularly relevant to 6206 given its increased susceptibility to alpha-defensins. Modified gentamicin protection assays were completed to assess the ability of these strains to invade the iHO epithelium. Strains 6206 and 6174 were also consistently less able to invade and survive within the iHO epithelial cells, with only 6206 being recoverable at 3 hours post-infection. Whilst P125109 was significantly more invasive than the other *S*. Enteritidis strains, intracellular counts at 3 hours remained lower than those for SL1344, suggesting that these *S*. Enteritidis are less able to adapt to the iHO environment than *S*. Typhimurium (**Figure 5.7**).

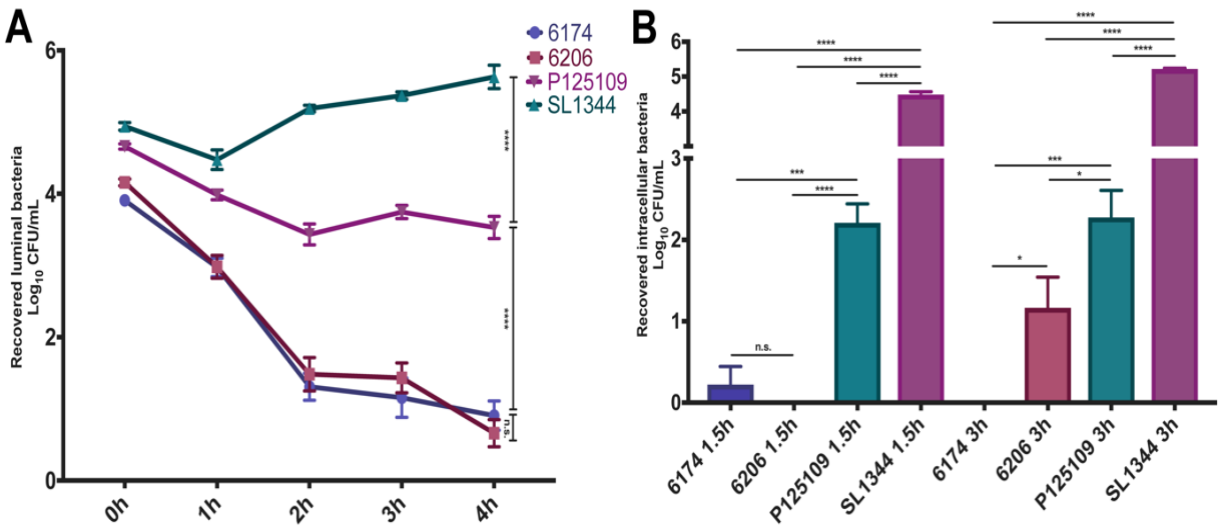

Figure 5.7: Recovered intraluminal and intracellular counts for *S.* Enteritidis in Kolf2 iHO. iHO were injected with S. Enteritidis 6174, 6206, P125109 or S. Typhimurium SL1344 and either incubated for 0, 1, 2, 3 or 4 hours, and luminal contents recovered (**A**), or incubated for 1.5 or 3 hours and modified gentamicin assays completed to recover intracellular bacteria (**B**). Data are presented for 3 biological replicates, (each averaged from 3 technical replicates) per condition +/- SEM. Multiple single iHO were used for luminal assays and 30 iHO injected per replicate for intracellular assays. Unpaired Mann-Whitney test was used to compare results (**n.s.** not significant, * p<0.05, ***p <0.001, ****p <0.0001). (**A**) Intraluminal counts from 0-4 hours post-infection. An initial decrease in recovered counts was observed for all strains, followed by recovery in SL1344, static counts in P125109 and continuous decrease in 6174 and 6206. (**B**) Intracellular counts show significantly more invasion in SL1344 and P125109, with no bacteria from strain 6174 invading and surviving until 3 hours post infection.

Given the large difference in luminal survival between the serovars of *Salmonella*, these assays were repeated using BRD948, an attenuated derivative of *S.* Typhi Ty2, with mutations in the *aroC* and *aroD* genes (responsible for aromatic amino acid biosynthesis[28]) and *htrA* (a serine protease required for virulence[29]). It was anticipated that this attenuated *S*. Typhi derivative would be less invasive than the virulent isolates previously tested, and should be present for longer in the iHO lumen. Luminal infection assays and modified gentamicin protection assays were carried out as previously described, with the exception that BRD948 required growth in LB broth supplemented with aromatic amino acids (Aro mix: phenylalanine 0.04 g/L, tryptophan 0.04 g/L, para-aminobenzoic acid 0.01 g/L and dihydro-oxbenzoic acid 0.01 g/L) and tyrosine 0.04 g/L. As predicted, numbers of recovered intracellular BRD948 were markedly lower; in this case ~3-log lower than those observed in previous assays with SL1344. Similarly, when harvesting iHO at the usual luminal timepoint of 1.5 hours, no viable bacteria remained, therefore assays were shortened and iHO harvested at 0, 20 and 40 minutes post-infection to check whether viable bacteria were present immediately following infection. By 40 minutes post-infection, intraluminal BRD948 counts were only 20% of those recovered at 0h (**Figure 5.8**). As an additional comparator,

these assays were completed for *S*. Typhimurium D23580, a multi-drug resistant ST313 isolate, known to cause invasive salmonellosis in sub-Saharan Africa,[30] in order to assess whether this isolate survived in the iHO prior to its use in experiments discussed later in the chapter. D23580 survived both intracellularly and in the lumen at higher counts than BRD948.

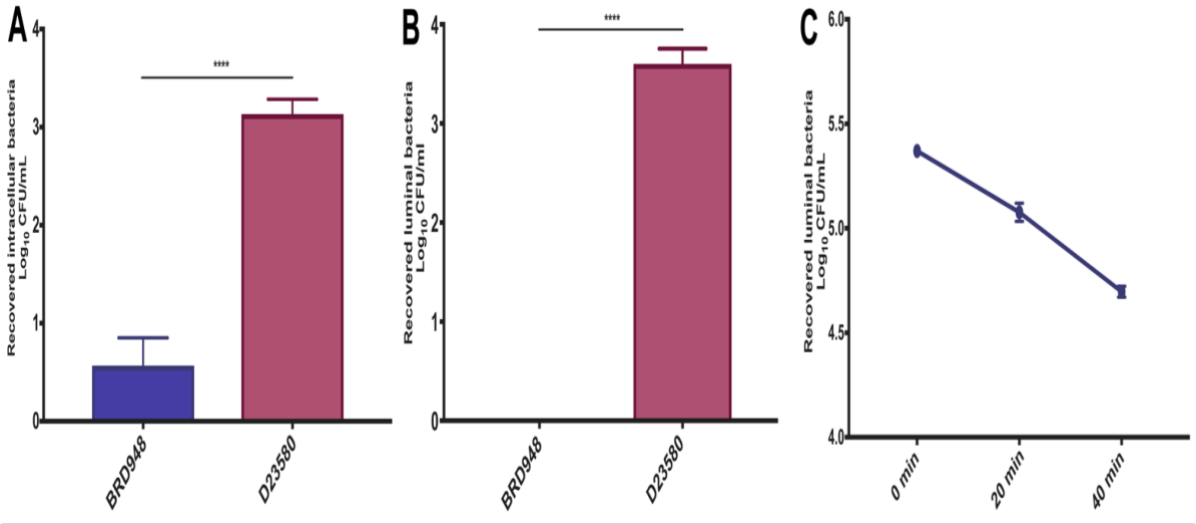

Figure 5.8: Recovered intraluminal and intracellular counts for *S*. Typhimurium D23580 and *S*. Typhi BRD948 in Kolf2 iHO. iHO were injected with S. Typhi BRD942 or S. Typhimurium D23580 and incubated for 1.5 hours, following which they underwent either modified gentamicin assay to recover intracellular bacteria (**A**) or recovery of luminal contents (**B**). Data presented are for 3 biological replicates (each averaged from 3 technical replicates), with 30 iHO injected per replicate, +/- SEM. Unpaired Mann-Whitney test was used to compare results (****p <0.0001). (**A**) Significantly more D23580 were recovered from inside enterocytes at 1.5 hours post-infection. (**B**) Intraluminal counts showed no recovery of BRD948 at 1.5 hours post-infection. Therefore, iHO were harvested at 0, 20 and 40 minutes following infection (**C**), which demonstrated a rapid drop in numbers of bacteria recovered by 40 minutes post-infection.

Given that intraluminal killing of bacteria was taking place with these 'less invasive' isolates, the question arose as to what would happen in the lumen to diarrhoeagenic bacterial strains which are non-invasive; preferentially existing in the lumen, such as Enteropathogenic *E. coli* (EPEC). In order to image these interactions, EPEC wild type isolate E2348/69 was transformed using electroporation with the TIMER^{bac} plasmid as described in 2.4. Intraluminal assays using single iHO and immunostaining following microinjection into iHO demonstrated a significant initial decrease in viable bacterial numbers retrieved from the iHO lumen, followed by some stabilisation of bacterial counts (**Figure 5.9**). Immunostaining was performed in order to try and determine whether the TIMER^{bac}-EPEC were producing attaching and effacing lesions on the iHO epithelium. It was not possible to clearly demonstrate these lesions, but immunostaining did reveal close interaction and apparent attachment of TIMER^{bac}-EPEC to the apical surface of the enterocytes.

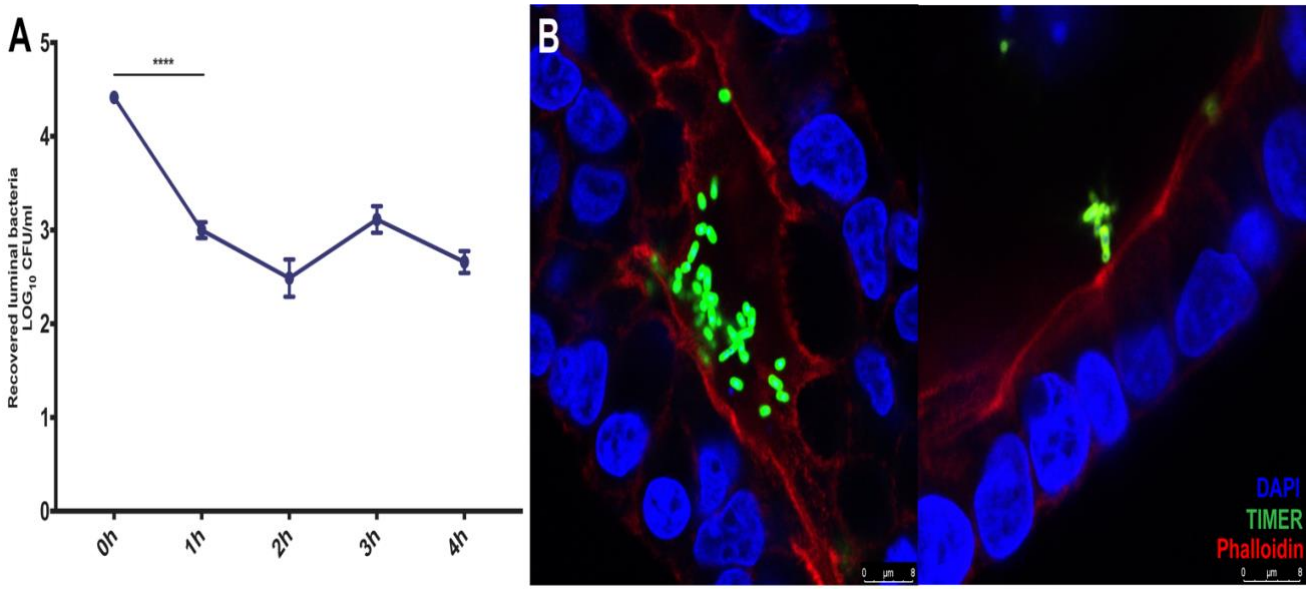

Figure 5.9: Recovered intraluminal counts for TIMER^{bac}-EPEC and immunostaining of interactions with the Kolf2 iHO epithelium. (**A**) iHO were injected with TIMER^{bac}-EPEC and luminal contents recovered at 0, 1, 2, 3 or 4 hours post-infection. Data presented are for 3 biological replicates (each averaged from 3 technical replicates) +/- SEM. Unpaired Mann-Whitney test was used to compare results (****p <0.0001). Intraluminal counts of recovered bacteria displayed a significant drop in initial viable counts followed by some stabilisation. (**B**) iHO were injected with TIMER^{bac}-EPEC and incubated for 3 hours prior to fixing and immunostaining for nuclei (DAPI) and epithelial brush border (phalloidin), which demonstrated TIMER^{bac}-EPEC interacting with the iHO epithelium. Images taken on the Leica SP8 confocal microscope at 63x magnification.

5.4 Other applications for the iHO model – study of competition between bacterial strains

There are a wide range of *Salmonella* capable of causing different types of disease in different hosts. *S*. Typhi are discussed in Chapter 6, but having assessed the survival of an invasive salmonellosis (iNTS) isolate in the iHO model, it was investigated as to how other 'invasive' *Salmonella* would behave in comparison to the *S*. Typhimurium reference isolate SL1344 if iHO were simultaneously infected by multiple isolates. Would the isolates causing the more severe disease picture outcompete those causing milder disease *in vitro*? To this end, as an initial comparator, TIMER^{bac}-*Salmonella* SL1344 were assayed in competition with *S*. Typhimurium D23580. As described in 2.3, modified gentamicin protection assays were completed, with results recorded for intracellular counts when each isolate was injected alone into the iHO, followed by both isolates in combination. The fluorescence demonstrated by the TIMER^{bac}-SL1344 colonies made it possible to distinguish easily between the two bacterial strains when colonies were counted at the end of the experiment. There was no significant difference in recovered counts of each isolate when injected separately into the iHO, but D23580 outcompeted the TIMER^{bac}- SL1344, with

significantly more D23580 being located intracellularly when both isolates were injected in equal ratios into the iHO (**Figure 5.10**). Mean competition index was 2.05 (SEM 0.31).

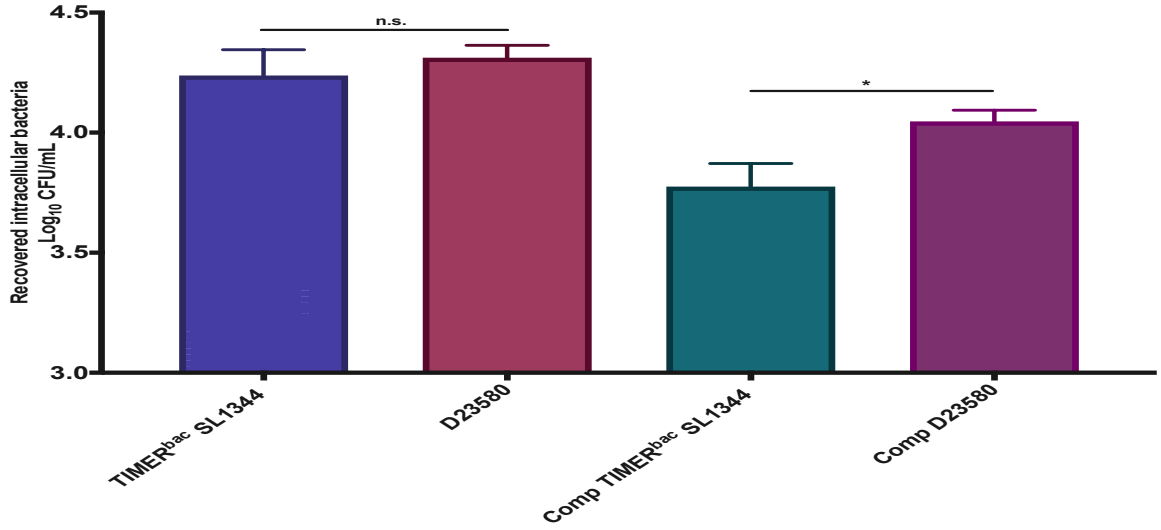

Figure 5.10: Recovered intracellular counts for TIMER^{bac}-*Salmonella* SL1344 and D23580 alone and in competition. iHO were either injected with TIMER^{bac}-SL1344 or D23580 at 1.6 x 10^9 alone, or in competition at a 50:50 ratio and incubated for 1.5 hours, prior to undergoing modified gentamicin assay to recover intracellular bacteria. Data are presented for 3 biological replicates (each averaged from 3 technical replicates) +/- SEM. Unpaired Mann-Whitney test was used to compare results (**n.s.** not significant, *p <0.05). There was no significant difference between recovered intracellular counts of each strain when injected alone into Kolf2 iHO, however when injected together in competition, (Comp TIMER^{bac} / Comp D23580), significantly more D23580 were recovered from within cells.

This investigation into iNTS-causing isolates was continued by undertaking assays with 5 Vietnamese ST34 clinical isolates from the same BAPS (Bayesian analysis of population structure) cluster, which had been isolated from blood or stool of patients presenting with salmonelloses.[31] Full details of the isolates are provided in Table 3.1. Briefly, the collection comprised 3 bloodstream isolates, 2 of which had biphasic flagellae (VNB1779, VNB2140) and 1 monophasic (VNB2315), and 2 stool isolates; 1 biphasic (VNS20081) and 1 monophasic (VNS20101). Cefepime protection competition assays were completed for these isolates as outlined in 3.2, given their high levels of gentamicin resistance. The three biphasic isolates VNB1779, VNB2140 and VNS20081 were able to successfully outcompete TIMER^{bac}-SL1344, with mean competition indices (CI) ranging from 6.35-16.34. Of the monophasic *Salmonella*, the bloodstream isolate VNB2315 was less invasive than TIMER^{bac}-SL1344, with a CI of 0.64 and the stool isolate VNS20101 was similarly invasive with a CI of 1.15 (**Figure 5.11**). These assays demonstrate the utility of the iHO model for examining interactions between different bacteria within the iHO system, and could pave the way for

work looking at the interactions and competition between commensals and pathogenic bacteria.

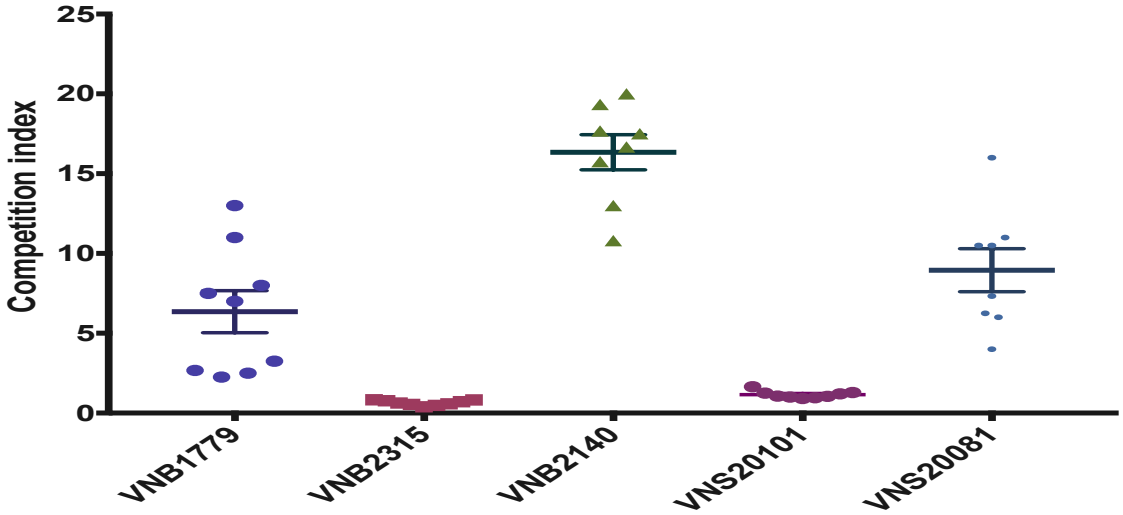

Figure 5.11: Competition indices for ST34 Salmonella versus TIMER^{bac}-*Salmonella* SL1344. Kolf2 iHO were injected with equal ratios of TIMER^{bac}-SL1344 and an ST34 strain and incubated for 1.5 hours prior to undergoing modified Cefepime protection assay and recovery of intracellular bacteria. Data are presented for 3 biological replicates (each averaged from 3 technical replicates) +/- SEM. ST34 isolates expressing biphasic flagellae were much more invasive than their monophasic counterparts; outcompeting TIMER^{bac}-SL1344 with 6 to 16-fold higher intracellular counts of recovered bacteria.

5.5 Other applications for the iHO model – investigating mutations of interest

One of the major advantages of hiPSC-derived iHO is the ability to produce models of the gut epithelium from individuals with disease-causing mutations without requiring an invasive biopsy. This approach facilitates studies on the function of the epithelium in diseased individuals compared to healthy controls. As an example, this project utilised hiPSC from an individual with a mutation in the CARD8 gene, a host gene with a role in the immune response to infection. CARD8 is an inhibitor of the pro-inflammatory protein, caspase-1. CARD8 and other CARD-containing proteins regulate apoptosis via interaction with caspases and control activation of the NF-κB pathway, modulating expression of genes involved in inflammation.[32] CARD8 has no murine homolog. Mutations in CARD8 can lead to loss of inhibition of NF-κB mediated signalling and a clinical phenotype of auto-inflammation and immune dysregulation, including an association with systemic inflammatory response syndrome in human studies.[33] There is debate about where exactly CARD8 fits in with the inflammasome, with some studies suggesting that CARD8 directly

interacts with capsase-1 through a CARD-CARD homophilic interaction, negatively regulating the activation of caspase-1.[32] Others have suggested a model where the nucleotide binding oligomerization domain-like receptor 3 (NLRP3) inflammasome is made up of a complex of NLRP3, apoptosis-associated speck-like protein (ASC), caspase-1 and CARD8; having witnessed interactions between the FIIND domain of CARD8 and the NOD domain of NLRP3.[34] More recent studies have demonstrated that NLRP3 interacts with CARD8 in the resting state, but following stimulation with LPS, NLRP3 instead interacts with ASC, suggesting that CARD8 may hold NLRP3 in an inactive form until a certain stimulation threshold is reached.[35] It may well be that elements of both of these hypotheses are true, with CARD8 having been shown to interact with the NOD domain of NOD2 (an NLR protein), decreasing NOD2-mediated defence from *Listeria*, via inhibition of construction of the nodosome.[36] The outcome of these mechanisms is that CARD8 causes caspase-1 inhibition; resulting in decreased IL-1β levels, in addition to decreasing NF-κB signalling.[36] NF-κB-mediated signalling is also responsible for levels of IFNγ, IL-2, IL-6, IL-8 and β-interferon. Loss of function alleles in CARD8 have been reported to lead to increased cell death during *in vitro Salmonella* infections in lymphoblastoid cells.[33]

To investigate this potential phenotype of attenuated response to infection, hiPSC reprogrammed from a skin biopsy from a child with a mutation in the CARD8 gene were differentiated into iHO. This child had presented to paediatricians with unexplained multisystem inflammation and cirrhosis (medical history disclosed by T Kuijpers, Academic Medical Centre, Amsterdam). There was also evidence of 'immune dysregulation'; although the patient's primary humoral responses were normal, they had suboptimal immunologic memory function for Epstein-Barr virus and varicella-zoster virus and the presence of a number of autoantibodies. None of the child's direct relatives were similarly affected. Whole genome sequencing revealed a SNP causing a homologous missense mutation in an amino acid of the CARD8 gene (p.His280Tyr c.838C>T exon 7).

iHO generated from this individual were embedded and cultured as outlined in 2.1.2-2.1.4 (and are referred to henceforth as 'CARD8 cell line'). Light microscopy images taken during the differentiation process did not demonstrate any obvious differences between the CARD8 mutant line and the healthy control lines previously differentiated (**Figure 5.12**).

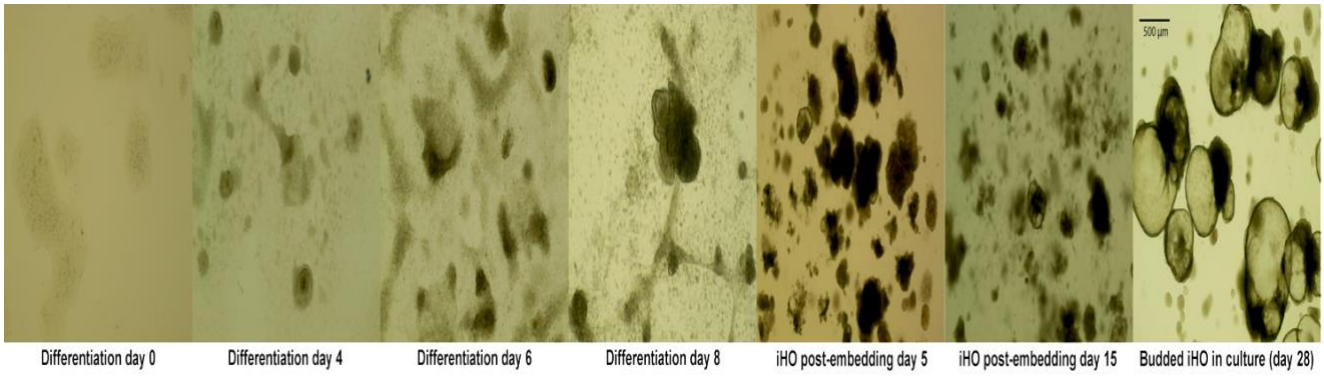

Figure 5.12: Sequential imaging of differentiation process for CARD8 cell line from hiPSC to iHO. Images taken on Thermo-Fisher EVOS XL imaging system at 4x (Differentiation and embedding panels) / 10x (iHO in culture) magnification.

CARD8 RNA and protein were previously shown to be expressed in haematopoietic cells and some gut tissue, including the small intestine.[37] On interrogation of the RNA-Seq data generated previously by Jessica Forbester on Kolf2 iHO, transcripts for CARD8 in intestinal epithelial cells were detected at a relatively low level. RNA was extracted from Kolf2 and CARD8 iPSC and iHO and RT-qPCR completed for genes of interest. There was no significant difference between the relative expression of the cell markers for iPSC or iHO from each cell line, although there was a trend towards higher lysozyme expression in CARD8 iHO versus Kolf2 iHO. Transcripts for CARD8 were expressed at low levels in all 4 conditions, suggesting that the commercial primers used were able to detect the transcript in both normal and mutant lines (**Figure 5.13**).

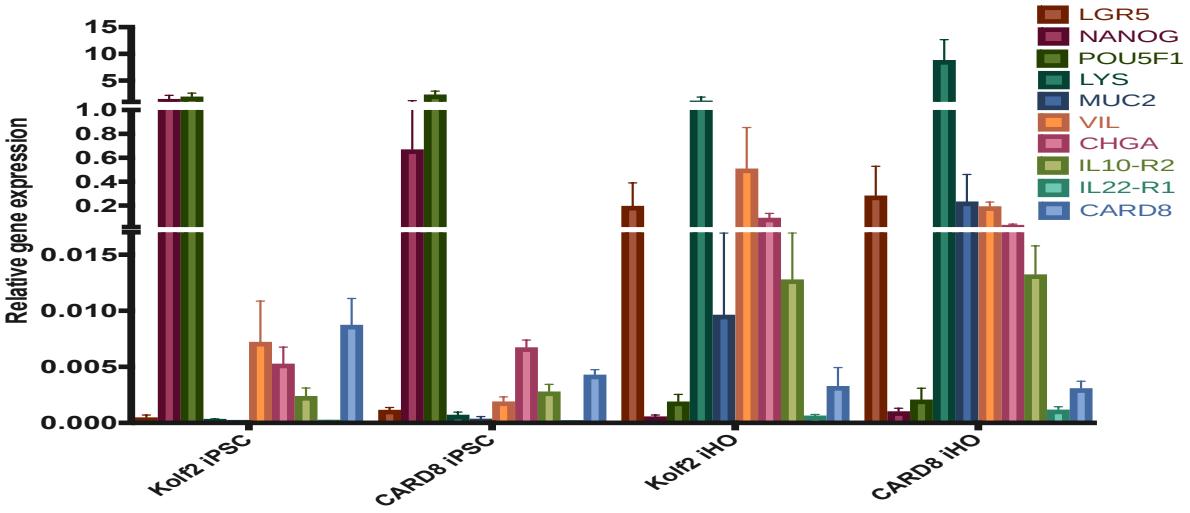

Figure 5.13: Expression of cell type markers in Kolf2 vs CARD8 iPSC and iHO. CARD8 transcripts appear to be expressed at low levels in both Kolf2 and CARD8 lines, with highest expression in Kolf2 iPSC. There are no significant differences in relative gene expression between the cell lines, although markers for Paneth cells appear to be more highly expressed in CARD8 iHO. Data presented are from 4 technical replicates, with assays repeated 3 times using paired iPSC/iHO of different batches. Data were analysed using the comparative cycle threshold (C_T) method, with GAPDH as an endogenous control. Unpaired Mann-Whitney test was used to compare results.

All expected cell type markers were visible on immunostaining, however the markers for secretory cell types (goblet cells, Paneth cells, enteroendocrine cells) appeared to be expressed at a relatively higher level in the CARD8 line (**Figure 5.14**).

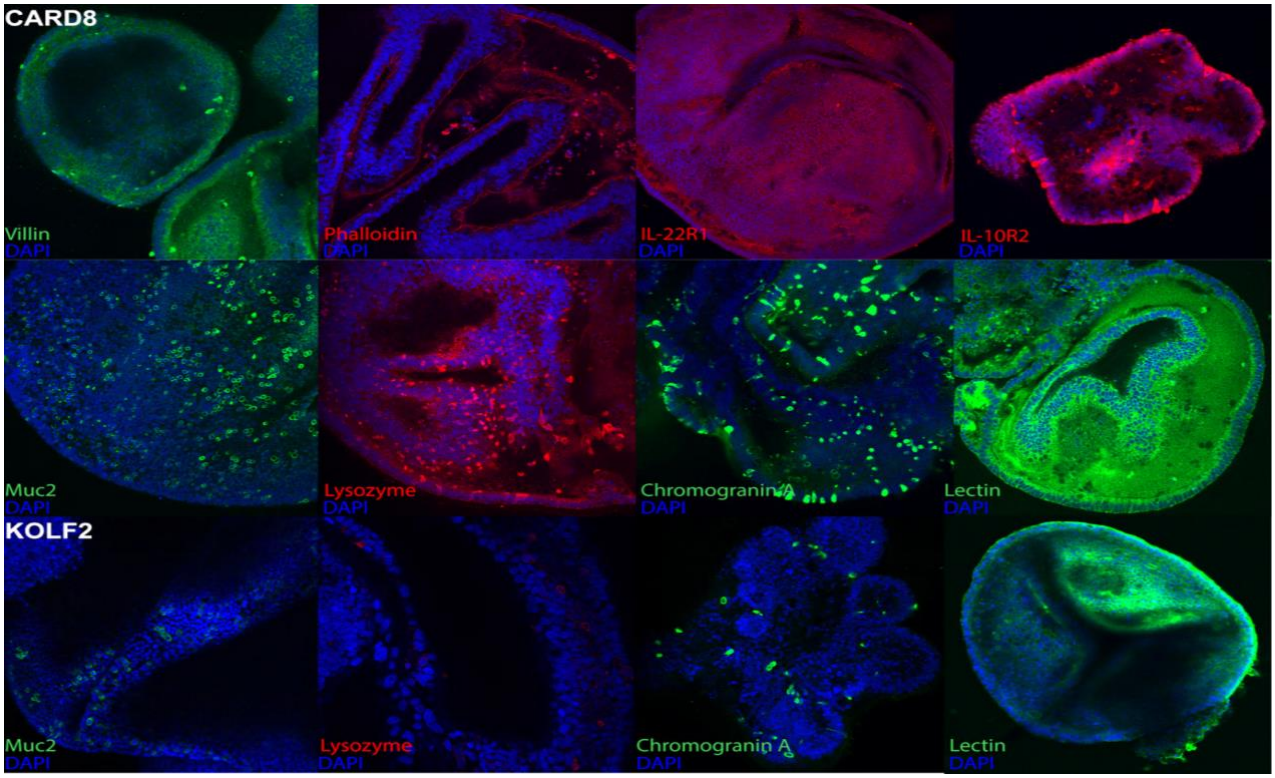

Figure 5.14: **Cell marker expression in iHO generated from CARD8 versus Kolf2 cell lines.** CARD8 iHO immunostaining demonstrates the presence of enterocytes (Villin), a polarised epithelium (Phalloidin) and components of the IL-22 receptor complex (IL-22R1, IL-10R2). Comparative to the Kolf2 iHO imaged in the lower panels, there are a relative abundance of goblet, Paneth and enteroendocrine cells in iHO from the CARD8 lineage (Muc2, Lysozyme, Chromogranin A respectively) and a well-formed mucus layer (Lectin). Images taken on Zeiss LSM 510 Meta confocal microscope at 20x magnification.

iHO from both lineages were then stained for the presence of the CARD8 protein, known to be expressed in both the nucleus and cytoplasm of cells.[37] Immunostaining again demonstrated the presence of the protein in iHO from both cell lines (**Figure 5.15**). The antibody used binds to the last 50 amino acids in the C-terminus of the CARD8 protein. Given the nature of the mutation (a mis-sense mutation, with single aa replacement), this portion of CARD8 protein may still be transcribed and translated.

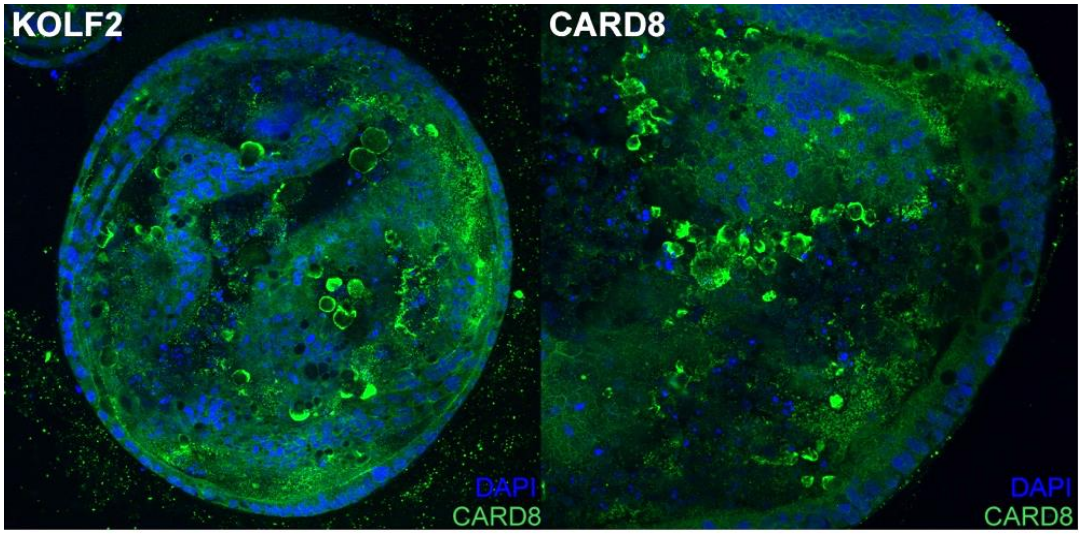

Figure 5.15: **CARD8 protein expression in CARD8 versus Kolf2 cell lines.** CARD8 immunostaining demonstrates the presence of CARD8 protein in iHO from both cell lines. Images taken on Zeiss LSM 510 Meta confocal microscope at 20x magnification.

Supernatants were taken from iHO of both Kolf2 and CARD8 lines microinjected with SL1344 and assayed for a number of cytokines. Previous data have shown decreased levels of circulating monocyte chemoattractant protein (MCP-1) associated with those with CARD8 polymorphisms and atherosclerotic disease[38]; our data showed an increased expression over time post-infection of MCP-1 in Kolf2 versus CARD8 iHO, but this was not significant (data not shown). Similarly, increase in IL-8 levels over time was greater in Kolf2 iHO, but this was again not significant due to lack of data points (data not shown). Western blots were completed for caspase-1 both pre-infection and after 1.5 and 3 hours post-infection with SL1344. Caspase-1 levels increased over time in the Kolf2 iHO, whereas in the CARD8 iHO caspase-1 levels decreased over time (**Figure 5.16**). This suggests that in the Kolf2 line, functional CARD8 protein may be binding to caspase-1 and inhibiting its activation and cleavage into active form.[32] Levels of caspase-1 thus increase, as production continues as part of the positive feedback loop in response to infection/inflammatory stimulus.[39] Whereas, in the CARD8 line, the lack of CARD8 allows processing and cleavage of caspase-1, and its autoprocessing, hence the decrease in levels over time.[32]

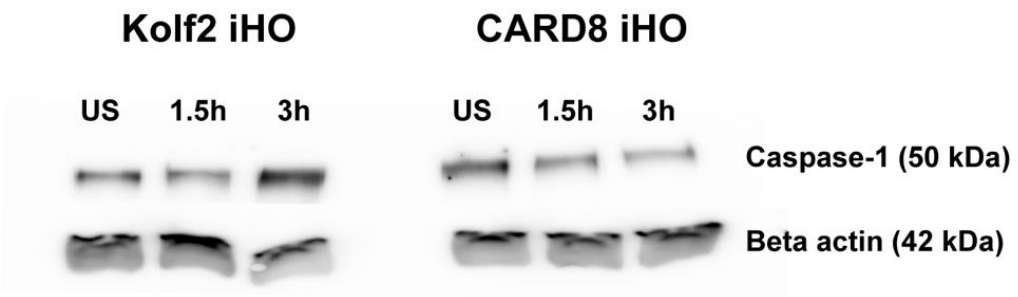

Figure 5.16: Western blot for caspase-1 using protein from unstimulated and infected iHO from Kolf2 and CARD8 lines. CARD8 and Kolf2 iHO were injected with SL1344, and harvested either prior to infection (US) or at 1.5 or 3 hours post-infection and protein extracted for western blotting for the presence of Caspase-1. Samples were also stained with anti-beta actin antibody to ensure equal protein loading across conditions. Images taken using ImageQuant LAS 4000. Increasing concentrations of caspase-1 are seen over time in Kolf2 iHO following infection, whereas the converse is seen in CARD8 iHO.

Given the interesting phenotypical differences seen using immunostaining and Western blotting, CARD8 iHO were microinjected with *S*. Typhimurium SL1344 to assess their susceptibility to infection versus their Kolf2 counterparts (**Figure 5.17**). These assays demonstrated significantly fewer bacteria invading intracellularly in the CARD8 iHO. Counts were lower at both 1.5 and 3 hours after infection, suggesting a decreased ability to invade and replicate intracellularly. It was hypothesised that bacteria may be being killed in the lumen by an increased concentration of antimicrobial peptides, given the higher proportion of Paneth cells suggested by staining in the CARD8 line. Therefore, luminal infection assays were done both in bulk and on sequentially harvested single iHO (**Figure 5.17**). Initial counts of SL1344 surviving in the lumen were similar for both cell lines, however at 3 hours, significantly more SL1344 were surviving and replicating in the lumen of the CARD8 iHO than the Kolf2 iHO. This was contrary to the expectation that more bacteria would be killed in the lumen by AMPs in the CARD8 iHO. However, it is worth noting that alongside the increased amount of Paneth cells in CARD8 iHO, there were also increased numbers of goblet cells and a more robust mucous layer, which may provide a protective environment for SL1344 to survive and replicate within in the lumen of the iHO (**Figure 5.18**). In addition, it is possible that the thicker mucus layer formed a physical barrier to prevent invasion, or that decreased intracellular invasion could be due to there being relatively fewer enterocytes versus secretory cells for the bacteria to invade through; given that epithelial invasion would be expected to occur via enterocytes (**Figure 5.17**).

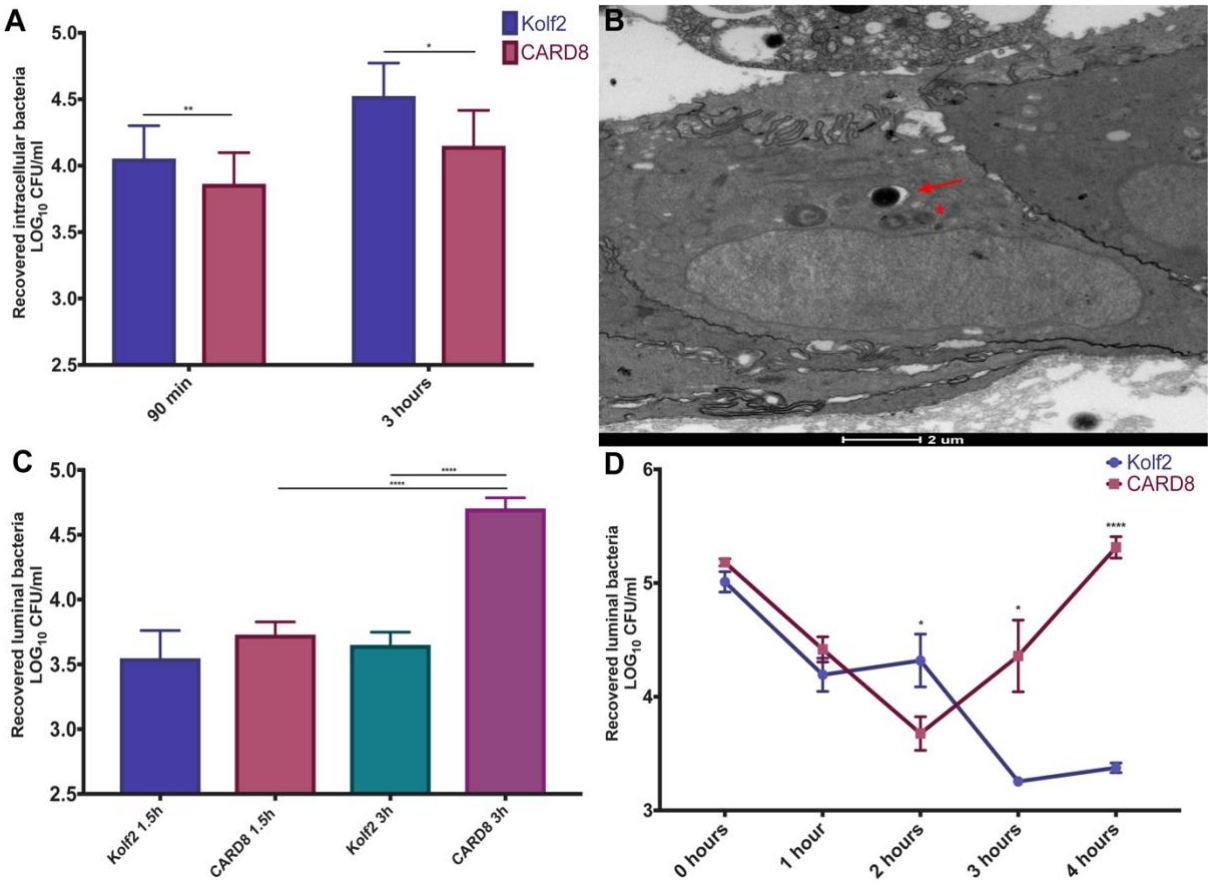

Figure 5.17: Intracellular and luminal bacterial counts in SL1344-infected Kolf2 and CARD8 iHO. (**A**) Kolf2 and CARD8 iHO were injected with SL1344 and incubated for 1.5 or 3 hours post-infection, followed by modified gentamicin protection assay to recover intracellular bacteria. Intracellular bacterial counts were lower in CARD8 iHO at both 1.5 and 3 hours. (**B**) TEM imaging of SL1344 bacteria inside of an enterocyte from CARD8 iHO at 1.5 hours post-infection, with bacteria located in SCV (arrow) and phagolysosome (asterisk). (**C**) Significantly more bacteria were recovered from the lumen of CARD8 versus Kolf2 iHO at 3 hours post-infection, with significant increase in the amount of bacteria between 1.5h and 3 hours in the CARD8 lumen. (**D**) Similar results were seen when single iHO were harvested at hourly intervals, with significantly more intraluminal bacteria being recovered from CARD8 iHO at 4 hours post infection. Data are presented for 3 biological replicates, (each averaged from 3 technical replicates) per condition +/- SEM. Multiple single iHO were used for luminal assays in **D** and 30 iHO injected per replicate for intracellular assays in **A** and luminal assays in **C**. Unpaired Mann-Whitney test was used to compare results (*p <0.05, **p<0.01, ****p<0.0001).

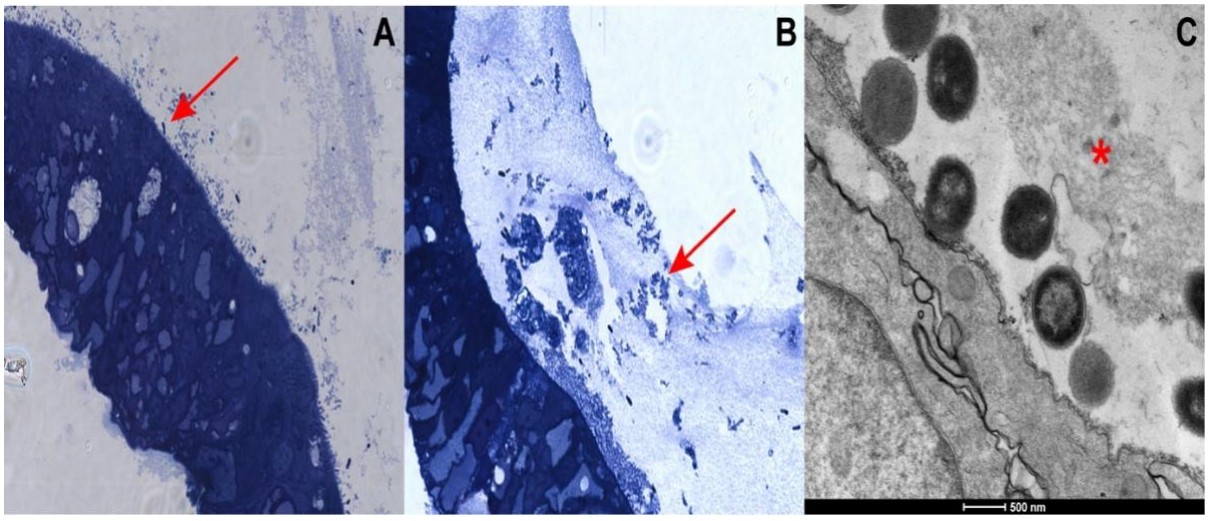

Figure 5.18: Bacterial interactions with the mucus layer following infection. Kolf2 and CARD8 iHO were injected with SL1344 and incubated for 1.5 hours prior to fixing and undergoing preparations for TEM. Toluidine blue staining demonstrates a thinner mucus layer in the Kolf2 iHO lumen (**A**), with more direct interaction between bacteria and epithelium (arrow), versus a thick mucus layer containing bacteria, seen in CARD8 iHO lumen (arrow) (**B**). Images taken at 63x magnification. (**C**) TEM imaging of SL1344 having breached the mucus layer (asterisk) and damaged microvilli on the apical surface of the epithelium in Kolf2 iHO.

5.6 Discussion

This chapter addresses a number of questions about the intraluminal environment of the iHO system, which is challenging to study. Ideally, obtaining material from the iHO lumen would involve a reverse microinjection system, and direct removal of luminal contents, since even breaking up iHO and releasing their luminal contents into small amounts of PBS will markedly dilute any peptides held within the lumen. Harvesting of cells and transcriptional analysis seemed an initial logical proxy as a method of making this measurement, but this would rely upon harvesting at the correct moment that each cytokine is being transcribed. The timing may, of course, differ amongst cytokines, which could explain why limited response was recorded amongst some of the AMPs studied in this chapter. Perhaps a later harvesting point and blotting for protein would have yielded additional data, as attempted in the mouse model described by Wilson et al.[3] This study notes restriction of *S.* Typhimurium LT2 strain growth in the lumen of murine organoids for up to 20 hours post infection due to alpha-defensin production, however, results presented at 9 hours post infection showed killing / growth restriction in some replicates and replication over the initial inoculum in others. In addition, the infective dose administered in these experiments was between 50 and 5000 CFU per organoid, versus ~17,000 CFU per iHO in this study, suggesting that there are sufficient defensin concentrations in the lumen to restrict growth of a small inoculum, but that this system can become overwhelmed with a larger infective dose, as seen in the current study.

It was curious to note that strains of *S*. Enteritidis, despite their ability to cause a similar clinical picture to *S*. Typhimurium of gastrointestinal disease and iNTS (even being recorded as a more common cause of invasive disease in some studies[11,40,41]), were much less successful at invading the epithelium. Both serovars harbour SPI-1 and SPI-2, so would be expected to have similar machinery for invading and replicating within cells.[40] None of the *S*. Enteritidis strains trialled in this study were known to have mutations in SPI-1 or SPI-2 genes. *S*. Enteritidis are known to have monophasic flagellae, as compared to *S.* Typhimurium SL1344 which is biphasic. The monophasic ST34 *S*. Typhimurium variants used in the competition model did however invade to a greater extent than *S.* Enteritidis, so it is unlikely that this is the sole cause of their limited invasion potential. Other outcomes of

genetic differences between *S*. Enteritidis and *S*. Typhimurium such as differing O antigens may have played a role in their ability to be recognised by an inflammatory response induced by the iHO epithelium. *S*. Enteritidis with outer membrane instabilities (such as antimicrobial peptide resistance gene mutations) were demonstrably less effective at colonising the avian intestine.[42] In this study, both *S*. Enteritidis 6206 and 6174 harboured membrane-related mutations, in addition to which, the *amiA* mutation in 6206 may have rendered it more sensitive to luminal AMP killing.

It was satisfying to witness the survival of EPEC within the iHO lumen. If time allowed, it would have been useful to obtain more detailed imaging, via TEM, of the interactions between the bacteria and the epithelial surface. This could clarify whether A/E lesions are being formed, and allow study of survival of mutant strains of this bacteria, such as those with mutations in adhesins such as bundle forming pili and EspA filaments, which have been demonstrated to be key in brush border attachment.[43]

The results generated when clinical isolates of *Salmonella* were placed into competition with a reference strain produced evidence of the potential of the iHO model for investigating differences between native and invasive bacteria in the gut. They also demonstrated a possible role for biphasic flagellae in success at invading the epithelium and evading the antibacterial response in the iHO system. Assays performed using these strains in murine bone marrow-derived macrophages demonstrated the same pattern of increased invasiveness of the biphasic versus monophasic strains, greater release of IL-1β in supernatants and pyroptosis of macrophages following infection with biphasic strains (S. Baker, unpublished data). The isolates used here were all multiply drug-resistant, so it may be that the plasmids encoding AMR are partly responsible for their increased invasiveness. It would be useful to generate mutants of these strains lacking their MDR plasmids and observe whether there is still a difference between monophasic and biphasic serovars. High resolution TEM imaging may also provide information as to the nature of flagellin expression during interactions with the epithelium.

The CARD8 work outlined in this chapter demonstrates the potential of the iHO model for the non-invasive investigation of response to infection in patients with genetic mutations

causing immune dysregulation. There were some interesting phenotypical differences in iHO generated from the patient cell line, which correlated with a differing response to *S*. Typhimurium infection than that seen in the healthy volunteer cell lines used elsewhere in this project. It would be of interest to look at responses in macrophages generated from this stem cell line too, as their response to infection will likely differ; one would expect to see a caspase-1 dependent inflammatory pyroptosis in *Salmonella*-infected macrophages (also witnessed in dendritic cells) versus the caspase-1 independent apoptosis seen in epithelial cells.[44] Given their lack of inhibition of caspase-1, one may expect CARD8-deficient macrophages to undergo pyroptosis more quickly following infection. Caspase-1 deficient mice demonstrated increased susceptibility to invasive salmonellosis, suggesting that in vivo, controlled pyroptosis is a protective mechanism to prevent disseminated infection.[45,46] In the pilot experiments with the CARD8 cell line outlined in this chapter, the patient line was being compared to a healthy control line with a different genetic background, meaning that there is the possibility of other genetic sources of variance causing the unusual CARD8 iHO phenotype and response to infection. It was therefore planned to construct an isogenic control line with which to repeat these experiments; using CRISPR/Cas9 to reproduce the point mutation seen in the patient line in the Kolf2 hiPSC background. This however proved more challenging than expected and at the time of writing, only heterozygous mutants have been produced, with one allele edited to have the CARD8 mutation and one remaining wild type. Once a homozygous mutant is produced, this work could be taken forwards by repeating the assays outlined above, completing experiments to assess relative proportions of iHO epithelial cell death following infection and investigating more closely the luminal environment produced during infection in iHO from a cell line deficient in CARD8. It would also be interesting to produce macrophages from this cell line with which to perform invasion assays and imaging, transcriptomics and supernatant analysis to study differences in inflammatory response between cells expressing CARD8 versus those that do not.

References:

1. Huang JY, Sweeney EG, Sigal M, et al. Chemodetection and Destruction of Host Urea Allows Helicobacter pylori to Locate the Epithelium. *Cell Host Microbe.* 2015;18(2):147-156.
2. Schumacher MA, Feng R, Aihara E, et al. Helicobacter pylori-induced Sonic Hedgehog expression is regulated by NFkappaB pathway activation: the use of a novel in vitro model to study epithelial response to infection. *Helicobacter.* 2015;20(1):19-28.
3. Wilson SS, Tocchi A, Holly MK, Parks WC, Smith JG. A small intestinal organoid model of non-invasive enteric pathogen-epithelial cell interactions. *Mucosal Immunol.* 2015;8(2):352-361.
4. Bevins CL, Salzman NH. Paneth cells, antimicrobial peptides and maintenance of intestinal homeostasis. *Nat Rev Microbiol.* 2011;9(5):356-368.
5. Schlaermann P, Toelle B, Berger H, et al. A novel human gastric primary cell culture system for modelling Helicobacter pylori infection in vitro. *Gut.* 2016;65(2):202-213.
6. Ettayebi K, Crawford SE, Murakami K, et al. Replication of human noroviruses in stem cell-derived human enteroids. *Science.* 2016;353(6306):1387-1393.
7. Saxena K, Blutt SE, Ettayebi K, et al. Human Intestinal Enteroids: a New Model To Study Human Rotavirus Infection, Host Restriction, and Pathophysiology. *J Virol.* 2016;90(1):43-56.
8. Karve SS, Pradhan S, Ward DV, Weiss AA. Intestinal organoids model human responses to infection by commensal and Shiga toxin producing Escherichia coli. *PLoS One.* 2017;12(6):e0178966.
9. Heo I, Dutta D, Schaefer DA, et al. Modelling Cryptosporidium infection in human small intestinal and lung organoids. *Nat Microbiol.* 2018;3(7):814-823.
10. Garcez PP, Loiola EC, Madeiro da Costa R, et al. Zika virus impairs growth in human neurospheres and brain organoids. *Science.* 2016;352(6287):816-818.
11. Galanis E, Lo Fo Wong DM, Patrick ME, et al. Web-based surveillance and global Salmonella distribution, 2000-2002. *Emerg Infect Dis.* 2006;12(3):381-388.
12. Cepeda-Molero M, Berger CN, Walsham ADS, et al. Attaching and effacing (A/E) lesion formation by enteropathogenic E. coli on human intestinal mucosa is dependent on non-LEE effectors. *PLoS Pathog.* 2017;13(10):e1006706.

13. Hafza N, Challita C, Dandachi I, Bousaab M, Dahdouh E, Daoud Z. Competition assays between ESBL-producing E. coli and K. pneumoniae isolates collected from Lebanese elderly: An additional cost on fitness. *J Infect Public Health.* 2018;11(3):393-397.
14. Haiko J, Westerlund-Wikstrom B. The role of the bacterial flagellum in adhesion and virulence. *Biology (Basel).* 2013;2(4):1242-1267.
15. Macnab RM. Genetics and biogenesis of bacterial flagella. *Annu Rev Genet.* 1992;26:131-158.
16. McQuiston JR, Parrenas R, Ortiz-Rivera M, Gheesling L, Brenner F, Fields PI. Sequencing and comparative analysis of flagellin genes fliC, fljB, and flpA from Salmonella. *J Clin Microbiol.* 2004;42(5):1923-1932.
17. Silverman M, Simon M. Phase variation: genetic analysis of switching mutants. *Cell.* 1980;19(4):845-854.
18. Forbester JL, Goulding D, Vallier L, et al. Interaction of Salmonella enterica Serovar Typhimurium with Intestinal Organoids Derived from Human Induced Pluripotent Stem Cells. *Infect Immun.* 2015;83(7):2926-2934.
19. Claudi B, Sprote P, Chirkova A, et al. Phenotypic variation of Salmonella in host tissues delays eradication by antimicrobial chemotherapy. *Cell.* 2014;158(4):722-733.
20. Helaine S, Thompson JA, Watson KG, Liu M, Boyle C, Holden DW. Dynamics of intracellular bacterial replication at the single cell level. *Proc Natl Acad Sci U S A.* 2010;107(8):3746-3751.
21. Abshire KZ, Neidhardt FC. Growth rate paradox of Salmonella typhimurium within host macrophages. *J Bacteriol.* 1993;175(12):3744-3748.
22. Salzman NH, Ghosh D, Huttner KM, Paterson Y, Bevins CL. Protection against enteric salmonellosis in transgenic mice expressing a human intestinal defensin. *Nature.* 2003;422(6931):522-526.
23. Hill DR, Huang S, Nagy MS, et al. Bacterial colonization stimulates a complex physiological response in the immature human intestinal epithelium. *Elife.* 2017;6.
24. Ipinza F, Collao B, Monsalva D, et al. Participation of the Salmonella OmpD porin in the infection of RAW264.7 macrophages and BALB/c mice. *PLoS One.* 2014;9(10):e111062.

25. Sun S, Berg OG, Roth JR, Andersson DI. Contribution of gene amplification to evolution of increased antibiotic resistance in Salmonella typhimurium. *Genetics.* 2009;182(4):1183-1195.
26. Oguri T, Yeo WS, Bae T, Lee H. Identification of EnvC and Its Cognate Amidases as Novel Determinants of Intrinsic Resistance to Cationic Antimicrobial Peptides. *Antimicrob Agents Chemother.* 2016;60(4):2222-2231.
27. Thomson NR, Clayton DJ, Windhorst D, et al. Comparative genome analysis of Salmonella Enteritidis PT4 and Salmonella Gallinarum 287/91 provides insights into evolutionary and host adaptation pathways. *Genome Res.* 2008;18(10):1624-1637.
28. Tacket CO, Hone DM, Curtiss R, 3rd, et al. Comparison of the safety and immunogenicity of delta aroC delta aroD and delta cya delta crp Salmonella typhi strains in adult volunteers. *Infect Immun.* 1992;60(2):536-541.
29. Lewis C, Skovierova H, Rowley G, et al. Salmonella enterica Serovar Typhimurium HtrA: regulation of expression and role of the chaperone and protease activities during infection. *Microbiology.* 2009;155(Pt 3):873-881.
30. Kingsley RA, Msefula CL, Thomson NR, et al. Epidemic multiple drug resistant Salmonella Typhimurium causing invasive disease in sub-Saharan Africa have a distinct genotype. *Genome Res.* 2009;19(12):2279-2287.
31. Mather AE, Phuong TLT, Gao Y, et al. New Variant of Multidrug-Resistant Salmonella enterica Serovar Typhimurium Associated with Invasive Disease in Immunocompromised Patients in Vietnam. *MBio.* 2018;9(5).
32. Razmara M, Srinivasula SM, Wang L, et al. CARD-8 protein, a new CARD family member that regulates caspase-1 activation and apoptosis. *J Biol Chem.* 2002;277(16):13952-13958.
33. Ko DC, Shukla KP, Fong C, et al. A genome-wide in vitro bacterial-infection screen reveals human variation in the host response associated with inflammatory disease. *Am J Hum Genet.* 2009;85(2):214-227.
34. Agostini L, Martinon F, Burns K, McDermott MF, Hawkins PN, Tschopp J. NALP3 forms an IL-1beta-processing inflammasome with increased activity in Muckle-Wells autoinflammatory disorder. *Immunity.* 2004;20(3):319-325.

35. Ito S, Hara Y, Kubota T. CARD8 is a negative regulator for NLRP3 inflammasome, but mutant NLRP3 in cryopyrin-associated periodic syndromes escapes the restriction. *Arthritis Res Ther.* 2014;16(1):R52.
36. von Kampen O, Lipinski S, Till A, et al. Caspase recruitment domain-containing protein 8 (CARD8) negatively regulates NOD2-mediated signaling. *J Biol Chem.* 2010;285(26):19921-19926.
37. Atlas HP. CARD8 - available from the Human Protein Atlas. 2019; https://www.proteinatlas.org/ENSG00000105483-CARD8/tissue. Accessed 24th June 2019.
38. Paramel GV, Folkersen L, Strawbridge RJ, et al. CARD8 gene encoding a protein of innate immunity is expressed in human atherosclerosis and associated with markers of inflammation. *Clin Sci (Lond).* 2013;125(8):401-407.
39. Lee DJ, Du F, Chen SW, et al. Regulation and Function of the Caspase-1 in an Inflammatory Microenvironment. *J Invest Dermatol.* 2015;135(8):2012-2020.
40. Alghoribi MF, Doumith M, Alrodayyan M, et al. S. Enteritidis and S. Typhimurium Harboring SPI-1 and SPI-2 Are the Predominant Serotypes Associated With Human Salmonellosis in Saudi Arabia. *Front Cell Infect Microbiol.* 2019;9:187.
41. Marder EP, Cieslak PR, Cronquist AB, et al. Incidence and Trends of Infections with Pathogens Transmitted Commonly Through Food and the Effect of Increasing Use of Culture-Independent Diagnostic Tests on Surveillance - Foodborne Diseases Active Surveillance Network, 10 U.S. Sites, 2013-2016. *MMWR Morb Mortal Wkly Rep.* 2017;66(15):397-403.
42. McKelvey JA, Yang M, Jiang Y, Zhang S. Salmonella enterica serovar enteritidis antimicrobial peptide resistance genes aid in defense against chicken innate immunity, fecal shedding, and egg deposition. *Infect Immun.* 2014;82(12):5185-5202.
43. Cleary J, Lai LC, Shaw RK, et al. Enteropathogenic Escherichia coli (EPEC) adhesion to intestinal epithelial cells: role of bundle-forming pili (BFP), EspA filaments and intimin. *Microbiology.* 2004;150(Pt 3):527-538.
44. Paesold G, Guiney DG, Eckmann L, Kagnoff MF. Genes in the Salmonella pathogenicity island 2 and the Salmonella virulence plasmid are essential for

Salmonella-induced apoptosis in intestinal epithelial cells. *Cell Microbiol.* 2002;4(11):771-781.

45. Fink SL, Cookson BT. Pyroptosis and host cell death responses during Salmonella infection. *Cell Microbiol.* 2007;9(11):2562-2570.

46. Lara-Tejero M, Sutterwala FS, Ogura Y, et al. Role of the caspase-1 inflammasome in Salmonella typhimurium pathogenesis. *J Exp Med.* 2006;203(6):1407-1412.